G. Lu, J. Zhang, L. Xiang, and X. Ge, “A Global Optimization Method for Energy-Minimal UAV-Aided Data Collection over Fixed Flight Path” accepted for presentation in *IEEE International Conference on Communications (ICC)*, Seoul, South Korea, May 2022.

A Global Optimization Method for Energy-Minimal UAV-Aided Data Collection over Fixed Flight Path

Guangping Lu[1], Jing Zhang[1], Lin Xiang[2], and Xiaohu Ge[1]
[1]School of Electronic Information and Communications, Huazhong University of Science and Technology
[2]Communications Engineering Lab, Technische Universität Darmstadt
Emails:{luguangping,zhangjing,xhge}@hust.edu.cn, l.xiang@nt.tu-darmstadt.de

***Abstract*—This paper considers optimal resource allocation for data collection from multiple ground devices (GDs) using a rotary-wing unmanned aerial vehicle (UAV). The UAV's flight *path*, i.e., the sequence of moving positions, is given *a priori* due to requirements of e.g. patrol and inspection missions, whereas the UAV's *trajectory*, i.e., the path and time schedule of movement, remains dependent on its hovering positions and flying speeds along the path. To improve the spectral and energy efficiency of the GDs, the UAV employs a directional antenna and performs wireless power transfer (WPT) to the GDs before collecting data from them. We jointly optimize the UAV's flying speeds, hovering locations, and radio resource allocation (including time, bandwidth and transmit power) for minimization of the total energy consumption of the UAV required for completing data collection along the flying path. We show that given any flight path, the propulsion energy consumption of the UAV is a convex function of the flight speeds. However, due to the highly directive transmission, communication and flight of the UAV become strongly coupled and complicates the problem, e.g. the selection of the UAV's hovering points will affect both the order of serving the GDs and the antenna gain of the UAV. Moreover, nonconvexity in the flight path constraints further obscures an efficient solution to the resource allocation problem. To tackle these challenges, we propose an iterative algorithm based on the branch-and-bound (BnB) method, which can obtain the globally optimal solution when the flight path coincides with the boundary of a convex set. Simulation results show that compared with several baseline algorithms, the proposed algorithm can significantly lower the energy consumption of the UAV during data collection.**

I. Introduction

Unmanned aerial vehicles (UAVs) can be rapidly deployed and dynamically reconfigured to provide short-term communication services, which has recently attracted significant interest in both academia and industry [1], [2]. To reap the benefits of UAV-aided communications, trajectory optimization is considered crucial and has been intensively investigated in a large body of literature; see e.g. [3], [4] and references therein. Most of these existing works usually consider *variable* flight path, where the sequence of moving positions can be dynamically adjusted at the time of flight. Consequently, full degrees of freedom (DoFs) can be achieved in optimizing the trajectories of the UAVs, i.e., the path and time schedule of movement.

The corresponding author is Prof. J. Zhang and the work is supported by the National Natural Science Foundation of China under Grant U2001210, Hubei Provincial Science and Technology Department under Grant 2021BAA009, partly supported by the postgraduate research funding of Huazhong University of Science and Technology under Grant YY202007. The work of L. Xiang has been funded by the LOEWE initiative (Hesse, Germany) within the emergenCITY center and has been supported by the BMBF project Open6GHub.

Other research works have also considered *fixed* flight paths for UAVs, which are planned *a priori*, before flights start [5], [6]. This is motivated by not only the requirements of specific UAV missions such as power line inspection and border patrol, but also the increasing concerns from the general public about safety and regulation of UAV flights, particularly in restricted air space. In particular, a large number of UAVs flying in the sky may increase the risk of collisions and cause considerable interference to each other [7], [8]. To enable secure UAV applications and convenient management of the air traffic, the flight paths of the UAVs may have to be planned ahead for approval even in the uncontrolled air space [9]. Consequently, to avoid catastrophic collisions and unpleasant channel impairment such as Doppler shifts caused by UAV's mobility, the UAVs in these applications usually have to adopt a fly-and-hover scheme, which can only adjust the flying velocities and/or hovering points. This unfavorably limits the DoFs for trajectory optimization and the performance of UAV-aided communication systems. Moreover, solving the resulting trajectory and resource allocation optimization becomes challenging, as the path constraints are usually nonconvex. These issues were not addressed in the literature yet.

This paper investigates spectral- and energy-efficient UAV-aided communications over fixed flight paths. We consider a rotary-wing UAV, which is deployed for wirelessly transferring power to and collecting data from e.g. Internet-of-things devices on the ground while flying over a fixed path. Different from traditional energy-efficient designs of cellular networks, e.g. [10]–[14], [23], UAVs typically face the stringent size, weight, and power (SWAP) limitations. To improve communications along the fixed flight path, the UAV is equipped with a directional antenna. Thereby, high-gain and highly directional beams can be shaped to overcome the path losses and interference of the communication links for wireless power transfer (WPT) and data collection. Hence, high spectral and energy efficiency can be simultaneously achieved even for ground devices (GDs) with simple transceiver hardware and limited battery [15], [16]. Note that directional antennas have recently been advocated for UAV communications in [17].

However, as the directional antenna equipped at the UAV has limited coverage for communication, it is necessary to intelligently adjust the UAV's hovering points (which in turn affect both the order of serving the GDs and the antenna gain of the UAV) and resource allocation, and minimize the

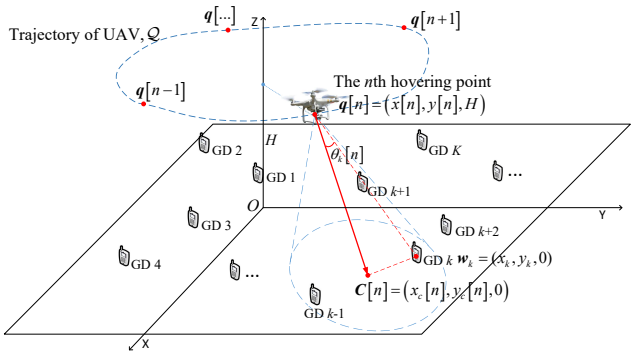

Fig. 1. UAV-aided wireless-powered data collection using directional antenna.

energy consumption of the UAV in order to reap the benefits of the considered system. This is difficult due particularly to the nonconvex constraint of fixed flight path. To address this challenge, we propose an iterative global optimization algorithm based on the branch-and-bound (BnB) method, which provides a performance benchmark for optimizing UAV flight and communications over fixed paths. We show that the proposed algorithm can obtain the globally optimal solution for the considered energy minimization problem when the given flight path is the boundary of its convex hull. Our contributions are

- We consider joint optimization of flight speeds, hovering locations, and radio resource allocation for energy-minimal UAV-assisted data collection using directional antenna. Unlike the existing literature, the UAV's flight path is given *a priori*.
- We propose a novel global optimization scheme based on the BnB method, which can optimally solve the formulated optimization problem under mild conditions.
- Simulation results show that the proposed scheme can efficiently adjust the hovering locations over the given flight path to significantly lower the total energy consumption of the UAV.

In the remainder of this paper, the system model is presented in Section II. The formulation and solution of the energy minimization problem are provided in Sections III and IV, respectively. Section V evaluates the performance of the proposed scheme via simulations and finally, Section VI concludes the paper.

II. System Model

A. Network Model

We consider a UAV-aided data collection system as in Fig. 1. A rotary-wing UAV is deployed to transmit power to and receive data from K GDs while patrolling along a predefined path. Let $\boldsymbol{K} = \{1, 2, ..., K\}$ be the index set of the GDs and $\boldsymbol{w}_k = (x_k, y_k, 0)$ be the location of GD $k \in \boldsymbol{K}$. Each GD has an energy harvesting circuit and a rechargeable battery, whereby energy is harvested from received radio frequency signals and stored for data transmission. The flight path, denoted by $\mathcal{Q}$, is a series of points to be sequentially reached by the UAV and has an overall length of L. The UAV performs WPT and data collection only during hovering.

Although confined to path $\mathcal{Q}$, the UAV can still flexibly select N points, indexed by set $\boldsymbol{N} = \{1, 2, ..., N\}$, from $\mathcal{Q}$ for hovering and adapt its flying velocities accordingly to optimize the fly-and-hover policy. Let $\boldsymbol{q}[n] = (x[n], y[n], H) \in \mathcal{Q}$ be the location of hovering point $n \in \boldsymbol{N}$, where the UAV keeps a fixed altitude, H. Accordingly, the GDs are divided into N groups, where the GDs in group $\boldsymbol{U}_n$ are served when the UAV hovers at point $\boldsymbol{q}[n]$. We assume that a GD can only be assigned to one group and each group is served by the UAV at one hovering point. The UAV aims to finish data collection from all GDs within time $T_{\max}$. Let t_n^f be the time duration for flying from point $\boldsymbol{q}[n-1]$ to $\boldsymbol{q}[n]$. Moreover, when hovering at $\boldsymbol{q}[n]$, the UAV spends two non-overlapping time intervals of duration t_n^w and t_n^u for WPT to and data collection from the GDs in $\boldsymbol{U}_n$, respectively.

B. Downlink WPT and Uplink Data Transmission

The UAV is equipped with a directional antenna to enable power-efficient far-field WPT and high-rate data communication. We consider a conic antenna element with antenna gain given by $G(\theta) = A_g \cos^m(\theta)$ [18], [19]. Here, A_g is the maximal antenna gain, $m \geq 1$ determines the directivity of the shaped beam, and $\theta \in [0, \pi/2]$ is the angle of incidence. However, due to limited coverage of the directional antenna, the UAV may have to dynamically adjust its antenna pointing for serving different groups of GDs. This adjustment can be conveniently enabled when the antenna is mounted on the UAV using e.g. a gimbal. We assume that the directional antenna keeps pointing towards point $\boldsymbol{C}[n] = (x_c[n], y_c[n], 0)$ on the ground, when the UAV hovers at $\boldsymbol{q}[n]$. Based on trigonometry, we have

$$\cos\theta_k[n] = \frac{\|\boldsymbol{q}[n]-\boldsymbol{C}[n]\|^2+\|\boldsymbol{q}[n]-\boldsymbol{w}_k\|^2-\|\boldsymbol{C}[n]-\boldsymbol{w}_k\|^2}{2\|\boldsymbol{q}[n]-\boldsymbol{C}[n]\|\,\|\boldsymbol{q}[n]-\boldsymbol{w}_k\|}. \quad (1)$$

In this paper, we assume that $\boldsymbol{C}[n]$ is given e.g. as the center of the locations of the GDs in each group, which can be conveniently calculated via searching for the smallest circle enclosing these GDs, cf. [20, Theorem 2.1]. Consequently, $\cos\theta_k[n]$ in (1) and the resulting antenna gain of the UAV will only be affected by the hovering point $\boldsymbol{q}[n]$.

As the UAV is elevated, it can establish line-of-sight (LoS) connections to the GDs with high likelihood [22]. Hence, we consider quasi-static channel models for the uplink data collection and downlink WPT. Thereby, the channel power gains between GD k and the UAV for WPT and data collection remain constant while hovering at $\boldsymbol{q}[n]$ and are given by [21]

$$g_k[n] = \frac{\lambda^2 \kappa_{kn} A_g \cos^m\theta_k[n]}{(4\pi)^2\|\boldsymbol{q}[n]-\boldsymbol{w}_k\|^2}, k \in \boldsymbol{U}_n, n \in \boldsymbol{N}, \quad (2)$$

$$h_k[n] = \frac{\beta_0 \varphi_{kn} A_g \cos^m\theta_k[n]}{\|\boldsymbol{q}[n]-\boldsymbol{w}_k\|^2}, k \in \boldsymbol{U}_n, n \in \boldsymbol{N}, \quad (3)$$

respectively, where λ is the carrier wavelength. κ_{kn} and φ_{kn} denote the channel fading. β_0 is the channel path loss at a reference distance of $d_{\text{ref}} = 1$ m.

The energy received at GD k in group $\boldsymbol{U}_n$ during WPT is

$$E_k^{\text{WPT}}[n] = \eta P_{\text{WPT}}[n] g_k[n] t_n^w, \; k \in \boldsymbol{U}_n, n \in \boldsymbol{N}, \quad (4)$$

where $\eta \in (0,1)$ is the energy conversion efficiency of the energy harvesting circuits at the GDs and $P_{\rm WPT}[n]$ is the transmit power of the UAV for WPT. Meanwhile, assume that the GDs in $\boldsymbol{U}_n$ simultaneously upload their data to the UAV using the orthogonal frequency-division multiple access (OFDMA). The instantaneous achievable data rate by GD k during uplink transmission is given by

$$R_k[n] = B_k \log\left(1 + \frac{P_k[n]h_k[n]}{B_k\sigma^2}\right),\ k \in \boldsymbol{U}_n, n \in \boldsymbol{N}, \quad (5)$$

where B_k and $P_k[n]$ are the allocated frequency bandwidth and the instantaneous transmit power of GD k.

C. Energy Consumption of the UAV

Let $E_{\rm prop}$ and $E_{\rm hover}$ be the energy consumption of the UAV during flight and hovering, respectively. Herein, $E_{\rm prop}$ includes the aerodynamic propulsion energy for flying over path $\mathcal{Q}$. Let L_n and $V[n]$ be the path length and the average speed when flying from point $\boldsymbol{q}[n-1]$ to $\boldsymbol{q}[n]$, respectively, where $L_n = \int_{\boldsymbol{q}[n-1]}^{\boldsymbol{q}[n]} d\mathcal{Q} = V[n]t_n^f$. We have [22]

$$E_{\rm prop} = \sum\nolimits_{n=1}^{N} \Bigg[\frac{L_nP_0}{V[n]} + \frac{3L_nP_0V[n]}{{U_{\rm tip}}^2} + \frac{L_nd_0\rho sAV[n]^2}{2} + L_nP_i\left(\left(V[n]^{-4} + \tfrac{1}{4v_0^4}\right)^{1/2} - \tfrac{1}{2v_0^2}\right)^{1/2}\Bigg]. \quad (6)$$

where d_0 is the fuselage drag ratio, ρ is the air density, s is the rotor solidity, v_0 is the mean rotor-induced velocity during hovering, and $U_{\rm tip}$ is the tip speed of the rotor blade. In addition, $P_0 = \frac{\delta}{8}\rho sA\Omega^3R_{\rm rotor}^3$ and $P_i = (1+\tau)\frac{W^{3/2}}{\sqrt{2\rho A}}$, where δ denotes the profile drag coefficient, A denotes the rotor disc area, Ω denotes the blade angular velocity, $R_{\rm rotor}$ is the rotor radius, τ and W represent an incremental correction factor and the aircraft weight, respectively.

On the other hand, $E_{\rm hover}$ includes the energy consumed for both aerodynamic propulsion and communication during hovering, and is given by

$$E_{\rm hover} = \sum\nolimits_{n=1}^{N} \Big(P_{\rm hover}\left(t_n^w + t_n^u\right) + P_{\rm WPT}[n]t_n^w + P_{\rm sta\_uav}\left(t_n^w + t_n^u\right)\Big), \quad (7)$$

where $P_{\rm hover} = P_0 + P_i$ is the aerodynamic power consumption for hovering, cf. (6), and $P_{\rm sta\_uav}$ is the static power consumption of the UAV's communication circuits.

III. Problem Formulation

To prolong the lifetime of the UAV, we jointly optimize the UAV's trajectory[1] $\{\boldsymbol{q}[n], V[n]\}$ and resource allocation $\{t_n^w, t_n^u, B_k, P_{\rm WPT}[n], P_k[n]\}$ for minimization of its energy consumption over the flight path $\mathcal{Q}$. To this end, we assume that the channel fading gains within time $T_{\max}$ are known. The resulting optimization problem is formulated as

$$\begin{aligned}
{\rm P1}: \min_{\substack{\boldsymbol{q}[n], V[n],\\ t_n^w, t_n^u, B_k, P_{\rm WPT}[n], P_k[n]}} \quad & E_{\rm prop} + E_{\rm hover} \\
{\rm s.t.}\ \ & C_1: \boldsymbol{q}[n] \in \mathcal{Q}, n \in \boldsymbol{N} \\
& C_2: \int_{\boldsymbol{q}[n-1]}^{\boldsymbol{q}[n]} d\mathcal{Q} = V[n]t_n^f, n \in \boldsymbol{N} \\
& C_3: 0 \le V[n] \le V_{\max}, n \in \boldsymbol{N} \\
& C_4: 0 \le P_{\rm WPT}[n] \le P_{\rm WPT}^{\max}, n \in \boldsymbol{N} \\
& C_5: 0 \le P_k[n] \le P_{k,\max}, k \in \boldsymbol{U}_n, n \in \boldsymbol{N} \\
& C_6: \sum\nolimits_{k\in\boldsymbol{U}_n} B_k \le B, n \in \boldsymbol{N} \\
& C_7: R_k[n] \ge R_{k,\min}, k \in \boldsymbol{U}_n, n \in \boldsymbol{N} \\
& C_8: t_n^u \ge D_k/R_k[n], k \in \boldsymbol{U}_n, n \in \boldsymbol{N} \\
& C_9: P_{\rm WPT}[n]g_k[n] \ge P_{k,\min}, k \in \boldsymbol{U}_n, n \in \boldsymbol{N} \\
& C_{10}: E_k^{\rm WPT}[n] \ge \left(P_k[n] + P_{\rm sta_user}\right)D_k/R_k[n], \forall k, n \\
& C_{11}: \sum\nolimits_{n=1}^{N} \left(t_n^f + t_n^w + t_n^u\right) \le T_{\max}. \quad (8)
\end{aligned}$$

In problem P1, constraint C_1 requires the UAV's hovering points to be on path $\mathcal{Q}$. C_2 specifies the path lengths between adjacent hovering points. C_3 limits the UAV's maximum velocity by $V_{\max}$. C_4, C_5 and C_6 limit the maximum transmit power of the UAV and the GDs, and the available frequency bandwidth, respectively. C_7 denotes the minimum rate requirements of the GDs. C_8 requires all data transmission from the GDs in group $\boldsymbol{U}_n$ to be completed within time t_n^u, where GD k transmits data of size D_k bits. C_9 requires a minimum received power of $P_{k,\min}$ at each GD during WPT, to activate the energy-harvesting circuit. C_{10} ensures that for each GD, the total energy consumed for data transmission does not exceed that received from the UAV for causal energy use. Finally, C_{11} requires the entire mission to be completed within time $T_{\max}$.

Problem P1 is a nonconvex optimization problem, where constraints C_1 and C_2 are nonconvex as $\mathcal{Q}$ is usually a nonconvex set. Moreover, as the transmit power of the UAV and the ground devices, i.e., $P_{\rm WPT}[n]$ and $P_k[n]$, are coupled with the antenna pointing direction, $\theta_k[n]$, or the time allocations, t_n^u and t_n^w, the objective function and the constraint functions in $C_7 \sim C_{10}$ are both nonconvex. This type of problem is generally NP-hard.

IV. Problem Solution

In this section, we first present the optimality conditions for problem P1. Using these results, we then show that when $\mathcal{Q}$ locates on the boundary of its convex hull, P1 can be optimally solved based on our proposed BnB algorithm.

A. Necessary Optimality Conditions

Lemma 1: Given any two hovering points $\boldsymbol{q}[n-1], \boldsymbol{q}[n] \in \mathcal{Q}$, the propulsion energy required by the UAV for flying from $\boldsymbol{q}[n-1]$ to $\boldsymbol{q}[n]$ along $\mathcal{Q}$, denoted as $E_{\rm prop}[n]$, is a convex function of the flight speed $V[n]$. Moreover, given any path $\mathcal{Q}$, the optimal flying speeds satisfy $V^*[n] = V^*[m], \forall n, m \in \boldsymbol{N}$.

[1] In this paper, we assume that the user groups $\boldsymbol{U}_n$, $n \in \boldsymbol{N}$ are given. However, the order of serving these groups will be optimized by sorting all hovering points $\boldsymbol{q}[n]$, $n \in \boldsymbol{N}$ on path $\mathcal{Q}$.

Proof: Based on (6), the UAV's propulsion energy consumption is given as $E_{\text{prop}}[n] = f_1(V[n]) + f_2(V[n])$, where

$$f_1(V[n]) = \frac{L_n P_0}{V[n]} + 3\frac{L_n P_0 V[n]}{{U_{\text{tip}}}^2} + \frac{1}{2} L_n d_0 \rho s A V[n]^2,$$

$$f_2(V[n]) = L_n P_i \left(\left(V[n]^{-4} + \frac{1}{4{v_0}^4} \right)^{1/2} - \frac{1}{2{v_0}^2} \right)^{1/2}. \quad (9)$$

Note that the path length $L_n = \int_{\boldsymbol{q}[n-1]}^{\boldsymbol{q}[n]} d\mathcal{Q}$ is fixed for given $\boldsymbol{q}[n-1]$ and $\boldsymbol{q}[n]$. Hence, $f_1(V[n])$ is a convex function of $V[n]$ for $V[n] > 0$. Moreover, we can show that $f_2''(V[n]) > 0$. Therefore, $f_2(V[n])$ and $E_{\text{prop}}[n]$ are convex with respect to $V[n]$. This further implies that

$$E_{\text{prop}} = \sum\nolimits_{n=1}^{N} E_{\text{prop}}[n] \overset{\text{(a)}}{\geq} \left[\frac{P_0}{\bar{V}} + 3\frac{P_0 \bar{V}}{{U_{\text{tip}}}^2} + \frac{1}{2} d_0 \rho s A \bar{V}^2 + P_i \left(\left(\bar{V}^{-4} + \delta^2 \right)^{\frac{1}{2}} - \delta \right)^{\frac{1}{2}} \right] \left(\sum\nolimits_{n=1}^{N} L_n \right), \quad (10)$$

where (a) follows from the Jensen's inequality, i.e., $\frac{1}{N}\sum_{n=1}^{N} f(V[n]) \geq f(\bar{V})$ and $\bar{V} = \frac{1}{N}\sum_{n=1}^{N} V[n]$. ■

Lemma 2: The optimal transmit powers of the UAV and the GDs during WPT and data transmission are given by $P_{\text{WPT}}^*[n] = P_{\text{WPT}}^{\max}$ and $P_k^*[n] = P_{k,\max}$, $\forall k \in \boldsymbol{U}_n, n \in \boldsymbol{N}$.

Proof: The proof is similar to that of [23, Lemma 2]. ■

Based on Lemmas 1 and 2, problem P1 can be equivalently reformulated as

$$\begin{aligned} \text{P2}: \min_{\boldsymbol{q}[n], V, t_n^u, t_n^w, B_k} \quad & E_c(V, t_n^u, t_n^w) \\ \text{s.t.} \quad & C_1, C_6 \sim C_{10}, \bar{C}_3 : 0 \leq V \leq V_{\max}, \\ & \bar{C}_{11} : \sum\nolimits_{n=1}^{N} (t_n^w + t_n^u) + L/V \leq T_{\max}. \end{aligned} \quad (11)$$

where $E_c(V, t_n^u, t_n^w) \triangleq E_{\text{prop}}(V) + \sum_{n=1}^{N} E_n(t_n^u, t_n^w)$ is the UAV's total energy consumption, and $E_n(t_n^u, t_n^w) \triangleq (P_{\text{hover}} + P_{\text{sta\_uav}})\, t_n^u + (P_{\text{WPT}}^{\max} A_{er} + P_{\text{hover}} + P_{\text{sta\_uav}})\, t_n^w$ is the UAV's energy consumption for serving group $\boldsymbol{U}_n$. $\bar{C}_{11}$ is due to $\sum_{n=1}^{N} t_n^f = \frac{L}{V}$, where $L = \sum_{n=1}^{N} L_n$. Problem P2 is still nonconvex due to the nonconvex constraints C_1, $C_7 \sim C_{10}$, but can be readily solved using the proposed BnB algorithm as will be explained below.

B. Proposed Solution of Problem P2

Assume that $\mathcal{Q}$ coincides with the boundary of its convex hull. Moreover, assume that the optimal hovering point $\boldsymbol{q}^*[n]$ lies in a candidate solution set or path segment $\mathcal{Q}^0[n] \triangleq [\underline{\boldsymbol{p}}^0[n], \overline{\boldsymbol{p}}^0[n]] \subseteq \mathcal{Q}$, where the end points of $\mathcal{Q}^0[n]$, i.e., $\underline{\boldsymbol{p}}^0[n]$ and $\overline{\boldsymbol{p}}^0[n]$ are given. The convex hull of $\mathcal{Q}^0[n]$, denoted as $\mathcal{R}^0[n]$, includes the region enclosed by the path segment $\mathcal{Q}^0[n]$ and the line segment from $\underline{\boldsymbol{p}}^0[n]$ to $\overline{\boldsymbol{p}}^0[n]$. Fig. 2 (a) illustrates $\mathcal{Q}^0[n]$ and $\mathcal{R}^0[n]$ in red dotted line and shaded area, respectively.

Let $j = 0, 1, \ldots$ be an iteration index. The proposed BnB algorithm consists of an iterative branching on all candidate solution sets, i.e., path segments $\mathcal{Q}^j[n], n \in \boldsymbol{N}$ possibly containing the optimal hovering points $\boldsymbol{q}^*[n]$, $n \in \boldsymbol{N}$. At each iteration j, we compute a lower bound (LB) and an upper bound (UB) on the optimal value, denoted as L^j and U^j, via search for relaxed hovering points in convex sets $\mathcal{R}^j[n] \subseteq \mathcal{R}^0[n], n \in \boldsymbol{N}$ and feasible hovering points in nonconvex sets $\mathcal{Q}^j[n], n \in \boldsymbol{N}$, respectively. By constructing $\mathcal{Q}^j[n] \subset \mathcal{Q}^{j-1}[n] \subset \ldots \subset \mathcal{Q}^0[n], \forall n \in \boldsymbol{N}$, the gap between the LBs and the UBs reduces iteratively until it vanishes, where the optimal solution is returned. In the following, we present the algorithm in three steps.

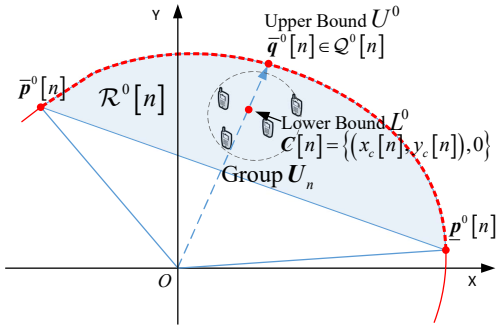

(a) Iteration $j = 0$, for Group $\boldsymbol{U}_n$

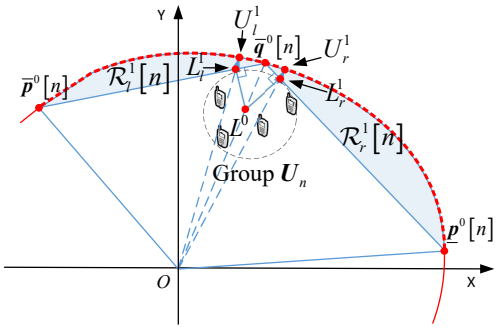

(b) Iteration $j = 1$, for Group $\boldsymbol{U}_n$

Fig. 2. Illustration of the proposed BnB algorithm for (a) iteration $j = 0$ and (b) $j = 1$.

1) Initial LB and UB ($j = 0$): To obtain an initial LB L^0 for problem P2, we first determine a relaxed hovering point $\underline{\boldsymbol{q}}^0[n]$. For this purpose, we replace constraint C_1 with $\boldsymbol{q}[n] = \underline{\boldsymbol{q}}^0[n] = (x_c[n], y_c[n], H)$. This reduces the path losses for all GDs during WPT and data collection, whereby the UAV's antenna is perpendicularly pointed to the ground and the incidence angle $\theta_k[n]$ satisfies

$$\cos\theta_k[n] = \frac{H}{\sqrt{H^2 + (x_c[n] - x_k)^2 + (y_c[n] - y_k)^2}}. \quad (12)$$

Consequently, the LB L^0 of problem P2 is given by the optimal value of the following problem, which is obtained by relaxing constraint C_1 as $\boldsymbol{q}[n] = \underline{\boldsymbol{q}}^0[n]$ and substituting $\cos\theta_k[n]$ in problem P2,

$$\begin{aligned} \text{P3}: \min_{V, t_n^w, t_n^u, B_k} \quad & E_c(V, t_n^u, t_n^w) \\ \text{s.t.} \quad & \bar{C}_3, C_6 \sim C_8, C_{10}, \bar{C}_{11}, \end{aligned} \quad (13)$$

Note that for given $\cos\theta_k[n]$, $C_6 \sim C_8$ and C_{10} in problem P3 are convex constraints. Hence, P3 is a convex problem.

On the other hand, to obtain an UB U^0 for problem P2, we project the hovering points $\underline{\boldsymbol{q}}^0[n], n \in \boldsymbol{N}$ onto $\mathcal{Q}^0[n]$, cf. Fig. 2(a), and the resulting feasible hovering point is denoted as $\overline{\boldsymbol{q}}^0[n], n \in \boldsymbol{N}$. The UAV can hover over point $\overline{\boldsymbol{q}}^0[n]$ and adjust the directional antenna to point toward $\boldsymbol{C}[n]$, where $\cos\theta_k[n]$ can be determined by substituting $\boldsymbol{q}[n] = \overline{\boldsymbol{q}}^0[n]$ into (1). Then, an UB of problem P2 can be obtained via solving problem P3 with $\overline{\boldsymbol{q}}^0[n]$ and the corresponding $\cos\theta_k[n]$.

2) Node Selection, Partitioning and Pruning: We use a search tree, denoted as $\mathcal{T}^j$ to keep track of all possible path segments containing the optimal hovering points $\boldsymbol{q}^*[n]$, $n \in \boldsymbol{N}$, at iteration j, which are included as nodes of $\mathcal{T}^j$. For initialization, we set $\mathcal{T}^0 = \{\mathcal{Q}^0\}$, where $\mathcal{Q}^0 \triangleq \prod_{n=1}^N \mathcal{Q}^0[n]$ is the node of $\mathcal{T}^0$. After obtaining the feasible hovering points $\overline{\boldsymbol{q}}^0[n]$, $n \in \boldsymbol{N}$ in 1), we partition each path segment $\mathcal{Q}^0[n]$ into two, $[\underline{\boldsymbol{p}}^0[n], \overline{\boldsymbol{q}}^0[n]]$ and $[\overline{\boldsymbol{q}}^0[n], \overline{\boldsymbol{p}}^0[n]]$, and the resulting two new nodes are appended into $\mathcal{T}^1$.

At iteration $j \geq 1$, for each node $\mathcal{Q}^j \in \mathcal{T}^j$ with $\mathcal{Q}^j \triangleq \prod_{n=1}^N \mathcal{Q}^j[n]$ and $\mathcal{Q}^j[n] \triangleq [\underline{\boldsymbol{p}}^j[n], \overline{\boldsymbol{p}}^j[n]]$, we compute an LB and an UB similar to 1). Let $\Phi_L(\mathcal{Q}^j)$ and $\Phi_U(\mathcal{Q}^j)$ be the LB and UB for P2 over a given path segment $\mathcal{Q}^j$, which are obtained by searching for the relaxed and the feasible hovering points, denoted as $\underline{\boldsymbol{q}}^j[n]$, $n \in \boldsymbol{N}$, and $\overline{\boldsymbol{q}}^j[n]$, $n \in \boldsymbol{N}$, respectively. Then the overall LB and UB for iteration j, L^j and U^j, are chosen as the smallest values of $\Phi_L(\mathcal{Q}^j)$ and $\Phi_U(\mathcal{Q}^j)$ among all path segments $\mathcal{Q}^j \in \mathcal{T}^j$, respectively. Further, we partition the path segments of node $\mathcal{Q}^j_{\text{sel}}$ into $\prod_{n=1}^N \left([\underline{\boldsymbol{p}}^j[n], \overline{\boldsymbol{q}}^j[n]] \cup [\overline{\boldsymbol{q}}^j[n], \overline{\boldsymbol{p}}^j[n]]\right)$ and update tree $\mathcal{T}^{j+1}$ accordingly, where $\mathcal{Q}^j_{\text{sel}} \in \text{argmin}_{\mathcal{Q}}\{\Phi_L(\mathcal{Q}) | \mathcal{Q} \in \mathcal{T}^j\}$.

Note that, at each iteration $j = 0, 1, \ldots$, any node $\mathcal{Q} \in \mathcal{T}^j$ whose LB $\Phi_L(\mathcal{Q})$ exceeds the current smallest UB U^j can be promptly pruned or deleted for memory savings without loss of optimality, i.e., $\mathcal{T}^{j+1} = \mathcal{T}^j \backslash \{\mathcal{Q} | \Phi_L(\mathcal{Q}) > U^j\}$.

3) Update of LBs and UBs ($j \geq 1$): At iteration $j \geq 1$, to compute $\Phi_L(\mathcal{Q}^j)$ for each $\mathcal{Q}^j \in \mathcal{T}^j$, we can select the hovering points $\underline{\boldsymbol{q}}^j[n]$, $n \in \boldsymbol{N}$ for LB as follows,

$$\underline{\boldsymbol{q}}^j[n] = \underset{\boldsymbol{q}[n] \in \mathcal{R}^j[n]}{\arg\min} \left\| \boldsymbol{q}[n] - \boldsymbol{C}[n] \right\|, \quad n \in \boldsymbol{N}, \tag{14}$$

where $\mathcal{Q}^j = \prod_{n=1}^N \mathcal{Q}^j[n]$, $\mathcal{R}^j[n]$ is the convex hull of $\mathcal{Q}^j[n] = [\underline{\boldsymbol{p}}^j[n], \overline{\boldsymbol{p}}^j[n]]$. This is because the UAV will otherwise experience a larger path loss and consume more energy during WPT and data collection. Note that (14) is a convex problem, which can be conveniently solved exploiting the geometry. In particular, $\underline{\boldsymbol{q}}^j[n]$ is a projection of $\boldsymbol{C}[n]$ onto the convex set $\mathcal{R}^j[n]$, as shown in Fig. 2(b).

On the other hand, to compute $\Phi_U(\mathcal{Q}^j)$, we can set $\overline{\boldsymbol{q}}^j[n]$ as the projection of $\underline{\boldsymbol{q}}^j[n]$, $n \in \boldsymbol{N}$, onto path segments $\mathcal{Q}^j[n]$, $n \in \boldsymbol{N}$. Then $\Phi_L(\mathcal{Q}^j)$ and $\Phi_U(\mathcal{Q}^j)$ are given by the optimal values of problem P3, where $\cos\theta_k$ is calculated according to $\underline{\boldsymbol{q}}^j[n]$, $n \in \boldsymbol{N}$ and $\overline{\boldsymbol{q}}^j[n]$, $n \in \boldsymbol{N}$, respectively. The optimal solution to problem P2 is obtained when the difference between L^j and U^j vanishes or the search tree $\mathcal{T}^j$ becomes empty, where the algorithm converges. The overall solution procedure is summarized in Algorithm 1.

The proposed algorithm satisfies the following properties:

Algorithm 1 Proposed Algorithm for Solving Problem P2

1: **Initialization:** Set path segments $\mathcal{Q}^0[n] = [\underline{\boldsymbol{p}}[n], \overline{\boldsymbol{p}}[n]]$, such that $\boldsymbol{q}^*[n] \in \mathcal{Q}^0[n]$; set $\mathcal{Q}^0 = \prod_{n=1}^N \mathcal{Q}^0[n]$, search tree $\mathcal{T}^0 = \{\mathcal{Q}^0\}$, tolerance $\varepsilon > 0$, and iteration index $j = 0$
2: **Initial Bounds:** Compute L^0 by solving problem P3 with $\boldsymbol{q}[n] = \underline{\boldsymbol{q}}^0[n]$; Compute U^0 by solving problem P3 with $\boldsymbol{q}[n] = \overline{\boldsymbol{q}}^0[n]$
3: **while** $U^j - L^j \geq \varepsilon$ and $\mathcal{T}^j \neq \emptyset$ **do**
4: $j = j + 1$
5: **for** each node $\mathcal{Q}^j \in \mathcal{T}^j$ **do**
6: **Bounding:** Compute $\Phi_L(\mathcal{Q}^j)$ and $\Phi_U(\mathcal{Q}^j)$ by solving problem P3 with $\boldsymbol{q}[n] = \underline{\boldsymbol{q}}^j[n]$, cf. (14), and $\boldsymbol{q}[n] = \overline{\boldsymbol{q}}^j[n]$, respectively
7: Set $\overline{\boldsymbol{q}}^j = \{\overline{\boldsymbol{q}}^j[n]\}_{n=1}^N$, such that $\overline{\boldsymbol{q}}^j[n]$ leads to the smallest objective value, i.e., $\overline{\boldsymbol{q}}^j = \text{argmin}_{\overline{\boldsymbol{q}}^j \in \mathcal{Q}} E_c(V, t_n^u, t_n^w)$
8: **end for**
9: **Branching:** For node $\mathcal{Q}^j \in \arg\min\{\Phi_L(\mathcal{Q}) | \mathcal{Q} \in \mathcal{T}^j\}$, partition $\mathcal{Q}^j$ into $\prod_{n=1}^N \left([\underline{\boldsymbol{p}}^j[n], \overline{\boldsymbol{q}}^j[n]] \cup [\overline{\boldsymbol{q}}^j[n], \overline{\boldsymbol{p}}^j[n]]\right)$, and append the resulting new nodes into $\mathcal{T}^{j+1}$
10: Update L^j and U^j as the smallest values of $\Phi_L(\mathcal{Q}^j)$ and $\Phi_U(\mathcal{Q}^j)$ for all $\mathcal{Q}^j \in \mathcal{T}^j$, respectively
11: **Pruning:** $\mathcal{T}^{j+1} = \mathcal{T}^j \backslash \{\mathcal{Q} | \Phi_L(\mathcal{Q}) > U^j\}$
12: **end while**
13: **Output:** the global ε-optimal solution $\overline{\boldsymbol{q}}^j$

1) The branching process is bound improving, i.e., the LBs improve monotonically per iteration.
2) The subdivision process is exhaustive, i.e., the maximum lengths of all path segments $\mathcal{Q}^j[n]$, $n \in \boldsymbol{N}$, shrink to zero as j becomes large.
3) The bounding is consistent with branching, i.e., the gap between the UB and the LB, $U^j - L^j$, vanishes as j becomes large.

As a result, Algorithm 1 is guaranteed to converge in a finite number of iterations [25], [26].

It should be noted that our proposed algorithm mainly focus on the choice of hovering point and resource allocation. Therefore, it can also be utilized to the resource allocation of fixed-path UAV without implementing WPT.

V. Simulation Results

In this section, we evaluate the performance of the proposed algorithm via simulations. The simulation parameters are set according to Table I. We consider a circular flight path for the UAV with a radius of 50 meters, where the GDs are randomly and uniformly distributed in the area enclosed by the flight path. For performance comparison, two baseline schemes are also evaluated. For baseline scheme 1, the UAV transfers power to and collects data from only one GD at a time. For baseline scheme 2, the hovering point at the path is chosen as the nearest point to the center of each group of GDs.

Fig. 3 shows the total energy consumption of the UAV versus the number of GDs when the UAV flies at different altitudes. As can be observed, the UAV's energy consumption increases monotonically with the number of GDs. This is because on the one hand, more energy is needed by the GDs for data transmission, which in turn increases the energy consumption of the UAV during WPT. On the other hand, as the UAV's maximal transmit power is fixed, the UAV has

TABLE I
SIMULATION PARAMETER SETTINGS.

Total flight distance of the UAV, L	315 m
Flight altitude of the UAV, H	30 m
Maximum speed of the UAV, $V_{\max}$	35 m/s
System bandwidth, B	10 MHz
Channel power gain at reference distance, β_0	-30 dB
Noise power spectral density, σ^2	-110 dBm
Static power consumption of the UAV, $P_{\text{sta\_uav}}$	1 W
Data size of GD k, D_k	0.5 Mbits
Maximum WPT power of the UAV, $P_{\text{WPT}}^{\max}$	30 W
Maximal antenna gain, A_g	10 dB
Antenna directivity factor, m	1
Maximum transmit power of GD k, $P_{k,\max}$	50 mW
Energy conversion efficiency at GDs, η	1
Minimum data rate for GD k, $R_{k,\min}$	1 Mbps
Minimum received power for GD k, $P_{k,\min}$	1 mW

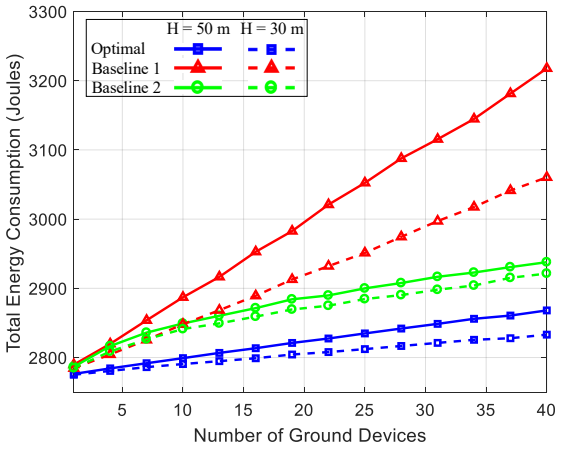

Fig. 3. Total energy consumption of the UAV versus the number of GDs.

to spend a longer time for WPT, which further increases the static energy consumption of the UAV. Fig. 3 also shows that compared with baseline schemes 1 and 2, our proposed scheme can significantly lower the energy consumption of the UAV, particularly when flying at a higer altitude. This is because unlike the baseline schemes, the proposed scheme can jointly optimize the hovering points, the bandwidth, time, and power resource allocation, and the antenna pointing direction, thereby utilizing more DoFs.

To evaluate the performance of UAV-aided communications, Fig. 4 evaluates the UAV's energy consumption during hovering versus the UAV's maximal transmit power for different numbers of GDs. We observe from Fig. 4 that for all considered schemes, the UAV's energy consumption always decreases with its transmit power, particularly when the number of GDs is large. This is because with higher transmit power at the UAV, the GDs can obtain the required energy in a shorter time during WPT. Consequently, the hovering time of the UAV is shortened, which reduces the UAV's energy consumption for communication. Meanwhile, as can be observed, compared with baseline schemes 1 and 2, the proposed scheme can substantially reduce the UAV's energy consumption for communication. For example, the proposed scheme achieves about 79% and 56% energy saving than baseline schemes 1 and 2 when $P_{\text{WPT}}^{\max}$ = 41 and 43 dBm

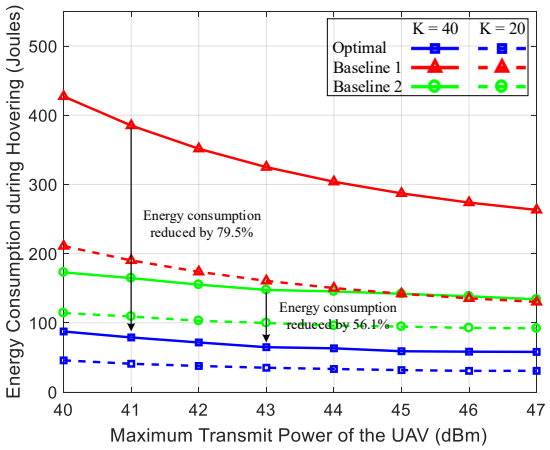

Fig. 4. Energy consumption during hovering versus the maximum transmit power of the UAV.

for K = 40, respectively.

VI. CONCLUSIONS

This paper investigated energy-minimal resource allocation for UAV-aided WPT and data collection from multiple GDs, where the UAV flies over a fixed flight path. We formulated a non-convex optimization problem for minimization of the total energy consumption of the UAV subject to constraints on flight path, communication quality of service, maximal transmit power, and time for completing the mission. Assuming that the flight path coincides with its convex hull, we further proposed a BnB-based algorithm to solve the formulated problem to optimality. Simulation results showed that the proposed BnB-based algorithm can significantly outperform several baseline schemes in terms of the energy consumption. In this work, we consider the condition that UAV's flight path locates on the boundary of its convex hull. Extending the recourse allocation framework to general flight path condition is an interesting topic for future research.

REFERENCES

[1] 3GPP TS 22.125, "Unmanned Aerial System (UAS) support in 3GPP," V17.3.0. [Online]. Avaliable: https://www.3gpp.org/DynaReport/22125.htm. Accessed on Apr. 02, 2021.

[2] H. Hellaoui, et al., "Aerial Control System for Spectrum Efficiency in UAV-to-Cellular Communications," *IEEE Commun. Mag.*, vol. 56, no. 10, pp. 108-113, Oct. 2018.

[3] M. Hua, et al., "3D UAV Trajectory and Communication Design for Simultaneous Uplink and Downlink Transmission," *IEEE Trans. Commun.*, vol. 68, no. 9, pp. 5908-5923, Sep. 2020.

[4] M. Mozaffari, et al., "A Tutorial on UAVs for Wireless Networks: Applications, Challenges, and Open Problems," *IEEE Commun. Surveys Tuts.*, vol. 21, no. 3, pp. 2334-2360, 3rd quarter 2019.

[5] Y. W. P. Hong, et al., "Power-Efficient Trajectory Adjustment and Temporal Routing for Multi-UAV Networks," *IEEE Trans. Green Commun. Netw.*, vol. 4, no. 4, pp. 1106-1119, Dec. 2020.

[6] H. Ye, et al., "Optimization for Full-Duplex Rotary-Wing UAV-Enabled Wireless-Powered IoT Networks," *IEEE Trans. Wireless Commun.*, vol. 19, no. 7, pp. 5057-5072, Jul. 2020.

[7] D. He, et al., "How to Govern the Non-Cooperative Amateur Drones?" *IEEE Netw.*, vol. 33, no. 3, pp. 184-189, May/Jun. 2019.

[8] E. Vinogradov, et al., "Wireless Communication for Safe UAVs: From Long-Range Deconfliction to Short-Range Collision Avoidance," *IEEE Veh. Technol. Mag.*, vol. 15, no. 2, pp. 88-95, Jun. 2020.

[9] M. Samir, et al., "UAV Trajectory Planning for Data Collection from Time-Constrained IoT Devices," *IEEE Trans. Wireless Commun.*, vol. 19, no. 1, pp. 34-46, Jan. 2020.
[10] X. Ge, et al., "User Mobility Evaluation for 5G Small Cell Networks Based on Individual Mobility Model," *IEEE J. Sel. Areas Commun.*, vol. 34, no. 3, pp. 528-541, Mar. 2016.
[11] X. Ge, et al., "Spatial Spectrum and Energy Efficiency of Random Cellular Networks," *IEEE Trans. Commun.*, vol. 63, no. 3, pp. 1019-1030, Mar. 2015.
[12] L. Xiang, et al., "Energy Efficiency Evaluation of Cellular Networks Based on Spatial Distributions of Traffic Load and Power Consumption," *IEEE Trans. Wireless Commun.*, vol. 12, no. 3, pp. 961-973, Mar. 2013.
[13] J. Zhang, et al., "Energy Efficiency Evaluation of Multi-Tier Cellular Uplink Transmission Under Maximum Power Constraint," *IEEE Trans. Wireless Commun.*, vol. 16, no. 11, pp. 7092-7107, Nov. 2017.
[14] J. Zhang, et al., "On the Performance of LTE/Wi-Fi Dual-Mode Uplink Transmission: Connection Probability Versus Energy Efficiency," *IEEE Trans. Veh. Technol.*, vol. 69, no. 10, pp. 11152-11168, Oct. 2020.
[15] S. Abeywickrama, et al., "Refined Nonlinear Rectenna Modeling and Optimal Waveform Design for Multi-User Multi-Antenna Wireless Power Transfer," *IEEE J. Sel. Areas Signal Process.*, vol. 15, no. 5, pp. 1198-1210, Aug. 2021.
[16] X. Chen, et al., "Wireless Energy and Information Transfer Tradeoff for Limited-Feedback Multiantenna Systems With Energy Beamforming," *IEEE Trans. Veh. Technol.*, vol. 63, no. 1, pp. 407-412, Jan. 2014.
[17] B. Yang, et al., "Performance, Fairness, and Tradeoff in UAV Swarm Underlaid mmWave Cellular Networks With Directional Antennas," *IEEE Trans. Wireless Commun.*, vol. 20, no. 4, pp. 2383-2397, Apr. 2021.
[18] Z. Wang, et al., "Wideband Frequency-domain and Space-domain Pattern Reconfigurable Circular Antenna Array," *IEEE Trans. Antennas Propag.*, vol. 65, no. 10, pp. 51795189, Oct. 2017.
[19] J. Zhang, et al., "On the Application of Directional Antennas in Multi-Tier Unmanned Aerial Vehicle Networks," *IEEE Access*, vol. 7, pp. 132095-132110, 2019.
[20] S. Xu, et al., "Solution methodologies for the smallest enclosing circle problem," *Comput. Optim. Appl.*, vol. 25, no. 1, pp. 283-292, 2003.
[21] T. D. P. Perera, et al., "Simultaneous Wireless Information and Power Transfer (SWIPT): Recent Advances and Future Challenges," *IEEE Commun. Surveys Tuts.*, vol. 20, no. 1, pp. 264-302, 1st quarter 2018.
[22] Y. Zeng, et al., "Energy Minimization for Wireless Communication With Rotary-Wing UAV," *IEEE Trans. Wireless Commun.*, vol. 18, no. 4, pp. 2329-2345, Apr. 2019.
[23] J. Zhang, et al., "Robust Energy-Efficient Transmission for Wireless-Powered D2D Communication Networks," *IEEE Trans. Veh. Technol.*, vol. 70, no. 8, pp. 7951-7965, Aug. 2021.
[24] M. Grant and S. Boyd, "CVX: Matlab software for disciplined convex programming," [Online] https://cvxr.com/cvx, Sep. 2013.
[25] F. Liu, et al., "Toward Dual-functional Radar-Communication Systems: Optimal Waveform Design," *IEEE Trans. Signal Process.*, vol. 66, no. 16, pp. 4264-4279, Aug. 2018
[26] H. Tuy, *Convex Analysis and Global Optimization*, Berlin, Germany: Springer, 2016.